

Density-functional-theory calculations of matter in strong magnetic fields. I. Atoms and molecules

Zach Medin and Dong Lai

*Center for Radiophysics and Space Research, Department of Astronomy,
Cornell University, Ithaca, New York 14853, USA*

(Received 9 June 2006; published 14 December 2006)

We present calculations of the electronic structure of various atoms and molecules in strong magnetic fields ranging from $B = 10^{12}$ G to 2×10^{15} G, appropriate for radio pulsars and magnetars. For these field strengths, the magnetic forces on the electrons dominate over the Coulomb forces, and to a good approximation the electrons are confined to the ground Landau level. Our calculations are based on the density functional theory, and use a local magnetic exchange-correlation function which is tested to be reliable in the strong field regime. Numerical results of the ground-state energies are given for H_N (up to $N = 10$), He_N (up to $N = 8$), C_N (up to $N = 5$), and Fe_N (up to $N = 3$), as well as for various ionized atoms. Fitting formulae for the B -dependence of the energies are also given. In general, as N increases, the binding energy per atom in a molecule, $|E_N|/N$, increases and approaches a constant value. For all the field strengths considered in this paper, hydrogen, helium, and carbon molecules are found to be bound relative to individual atoms (although for B less than a few $\times 10^{12}$ G, carbon molecules are very weakly bound relative to individual atoms). Iron molecules are not bound at $B \lesssim 10^{13}$ G, but become energetically more favorable than individual atoms at larger field strengths.

PACS numbers: 31.15.Ew, 95.30.Ky, 97.10.Ld

I. INTRODUCTION

Neutron stars (NSs) are endowed with magnetic fields far beyond the reach of terrestrial laboratories [1, 2, 3]. Most of the ~ 1600 known radio pulsars have surface magnetic fields in the range of $10^{11} - 10^{13}$ G, as inferred from their measured spin periods and period derivatives and the assumption that the spindown is due to magnetic dipole radiation. A smaller population of older, millisecond pulsars have $B \sim 10^8 - 10^9$ G. For about a dozen accreting neutron stars in binary systems, electron cyclotron features have been detected, implying surface fields of $B \sim 10^{12} - 10^{13}$ G. An important development in astrophysics in the last decade centered on the so-called anomalous x-ray pulsars and soft gamma repeaters [4]: there has been mounting observational evidence in recent years that supports the idea that these are magnetars, neutron stars whose radiations are powered by superstrong magnetic fields of order $10^{14} - 10^{15}$ G or higher [5, 6, 7]. By contrast, the highest static magnetic field currently produced in a terrestrial laboratory is 5×10^5 G; transient fields approaching 10^9 G have recently been generated during high-intensity laser interactions with dense plasmas [8].

It is well-known that the properties of matter can be drastically modified by strong magnetic fields found on neutron star surfaces. The natural atomic unit for the magnetic field strength, B_0 , is set by equating the electron cyclotron energy $\hbar\omega_{Be} = \hbar(eB/m_ec) = 11.577 B_{12}$ keV, where $B_{12} = B/(10^{12}$ G), to the characteristic atomic energy $e^2/a_0 = 2 \times 13.6$ eV (where a_0 is the Bohr radius):

$$B_0 = \frac{m_e^2 e^3 c}{\hbar^3} = 2.3505 \times 10^9 \text{ G.} \quad (1)$$

For $b = B/B_0 \gtrsim 1$, the usual perturbative treatment of the magnetic effects on matter (e.g., Zeeman splitting of atomic energy levels) does not apply. Instead, in the transverse direction (perpendicular to the field) the Coulomb forces act as a perturbation to the magnetic forces, and the electrons in an atom settle into the ground Landau level. Because of the extreme confinement of the electrons in the transverse direction, the Coulomb force becomes much more effective in binding the electrons along the magnetic field direction. The atom attains a cylindrical structure. Moreover, it is possible for these elongated atoms to form molecular chains by covalent bonding along the field direction. Interactions between the linear chains can then lead to the formation of three-dimensional condensed matter [9, 10, 11].

Our main motivation for studying matter in such strong magnetic fields arises from the importance of understanding neutron star surface layers, which play a key role in many neutron star processes and observed phenomena. Theoretical models of pulsar and magnetar magnetospheres depend on the cohesive properties of the surface matter in strong magnetic fields [12, 13, 14, 15, 16]. For example, depending on the cohesive energy of the surface matter, an acceleration zone (“polar gap”) above the polar cap of a pulsar may or may not form. More importantly, the surface layer directly mediates the thermal radiations from neutron stars. The advent of x-ray telescopes in recent years

has made detailed study of neutron star surface emission a reality. Such study can potentially provide invaluable information on the physical properties and evolution of NSs: equation of state at supernuclear densities, superfluidity, cooling history, magnetic field, surface composition, different NS populations, etc. (see, e.g., Ref. [17]). More than two dozen isolated neutron stars (including radio pulsars, radio-quiet neutron stars and magnetars) have clearly detected thermal surface emission [3, 18, 19]. While some neutron stars show featureless spectra, absorption lines or features have been detected in half a dozen or so systems [19]. Indeed, many of the observed neutron stars have sufficiently low surface temperatures and/or high magnetic fields, such that bound atoms or molecules are expected to be present in their atmospheres [20, 21, 22, 23]. It is even possible that the atmosphere is condensed into a solid or liquid form from which radiation directly emerges [11, 23, 24]. Thus, in order to properly interpret various observations of neutron stars, it is crucial to have a detailed understanding of the properties of atoms, molecules and condensed matter in strong magnetic fields ($B \sim 10^{11}\text{-}10^{16}$ G).

A. Previous works

H and He atoms at almost all field strengths have been well studied [10, 25, 26], including the nontrivial effect associated with the center-of-mass motion of a H atom [27]. Neuhauser *et al.* [28] presented numerical results for several atoms up to $Z = 26$ (Fe) at $B \sim 10^{12}$ G based on calculations using a one-dimensional Hartree-Fock method (see also Ref. [29] for Z up to 10). Some results [based on a two-dimensional (2D) mesh Hartree-Fock method] for atoms (up to $Z = 10$) at the field strengths $B/B_0 = 0.5 - 10^4$ are also available [30, 31, 32]. The Hartree-Fock method is approximate because electron correlations are neglected. Due to their mutual repulsion, any pair of electrons tend to be more distant from each other than the Hartree-Fock wave function would indicate. In zero-field, this correlation effect is especially pronounced for the spin-singlet states of electrons for which the spatial wave function is symmetrical. In strong magnetic fields ($B \gg B_0$), the electron spins (in the ground state) are all aligned antiparallel to the magnetic field, and the multielectron spatial wave function is antisymmetric with respect to the interchange of two electrons. Thus the error in the Hartree-Fock approach is expected to be less than the 1% accuracy characteristic of zero-field Hartree-Fock calculations [28, 33]. Other calculations of heavy atoms in strong magnetic fields include Thomas-Fermi type statistical models [34, 35, 36] and density functional theory [37, 38, 39, 40]. The Thomas-Fermi type models are useful in establishing asymptotic scaling relations, but are not adequate for obtaining accurate binding and excitation energies. The density functional theory can potentially give results as accurate as the Hartree-Fock method after proper calibration is made [41, 42].

Quantitative results for the energies of hydrogen molecules H_N with $N = 2, 3, 4, 5$ in a wide range of field strengths ($B \gg B_0$) were obtained (based on the Hartree-Fock method) by Lai *et al.* [11, 43] and molecular excitations were studied in Refs. [44, 45] (more complete references can be found in Ref. [11]). Quantum Monte Carlo calculations of H_2 in strong magnetic fields have been performed [46]. Some numerical results of He_2 for various field strengths are also available [11]. Hartree-Fock results of diatomic molecules (from H_2 up to C_2) and several larger molecules (up to H_5 and He_4) at $B/B_0 = 1000$ are given in Ref. [47].

B. Plan of this paper

In this paper and its companion paper [48], we develop a density-functional-theory calculation of the ground-state energy of matter for a wide range of magnetic field strengths, from 10^{12} G (typical of radio pulsars) to 2×10^{15} G (magnetar fields). We consider H, He, C, and Fe, which represent the most likely composition of the outermost layer of neutron stars (e.g., Ref. [3]). The present paper focuses on atoms (and related ions) and small molecules. Because of additional complications related to the treatment of band structure, calculations of infinite molecular chains and condensed matter are presented in Ref. [48].

Our calculations are based on density functional theory [49, 50, 51]. As mentioned above, the Hartree-Fock method is expected to be highly accurate, particularly in the strong field regime where the electron spins are aligned with each other. In this regime the density functional method is not as accurate, due to the lack of an exact correlation function for electrons in strong magnetic fields. However, in dealing with systems with many electrons, the Hartree-Fock method becomes increasingly impractical as the magnetic field increases, since more and more Landau orbitals (even though electrons remain in the ground Landau level) are occupied and keeping track of the direct and exchange interactions between electrons in various orbitals becomes computationally rather tedious. Our density-functional calculations allow us to obtain the energies of atoms and small molecules and the energy of condensed matter using the same method, thus providing reliable cohesive energy of condensed surface of magnetic neutron stars, a main goal of our study. Compared to previous density-functional-theory calculations [37, 38, 39, 40], we use an improved exchange-correlation function for highly magnetized electron gases, we calibrate our density functional code with previous

results (when available) based on other methods, and (for calculations of condensed matter) adopt a more accurate treatment of the band structure. Moreover, our calculations extend to the magnetar-like field regime ($B \sim 10^{15}$ G).

Note that in this paper we neglect the motions of the nuclei, due to electron-nucleus interactions or finite temperatures. The center-of-mass motions of the atoms and molecules induce the motional Stark effect, which can change the internal structure of the bound states (see, e.g., Refs. [11, 27]). Such issues are beyond the scope of this paper.

After summarizing the approximate scaling relations for atoms and molecules in strong magnetic fields in Sec. II, we describe our method in Sec. III and present numerical results in Sec. IV. Some technical details are given in the Appendix.

II. BASIC SCALING RELATIONS FOR ATOMS AND MOLECULES IN STRONG MAGNETIC FIELDS

A. Atoms

First consider a hydrogenic atom (with one electron and nuclear charge Z). In a strong magnetic field with $b = B/B_0 \gg Z^2$, the electron is confined to the ground Landau level (“adiabatic approximation”), and the Coulomb potential can be treated as a perturbation. The energy spectrum is specified by two quantum numbers, (m, ν) , where $m = 0, 1, 2, \dots$ measures the mean transverse separation between the electron and the nucleus ($-m$ is also known as the magnetic quantum number), while ν specifies the number of nodes in the z wave function. There are two distinct types of states in the energy spectrum $E_{m\nu}$. The “tightly bound” states have no node in their z wave functions ($\nu = 0$). The transverse size of the atom in the $(m, 0)$ state is $L_\perp \sim \rho_m = (2m + 1)^{1/2} \rho_0$, with $\rho_0 = (\hbar c/eB)^{1/2} = b^{-1/2}$ (in atomic units).¹ For $\rho_m \ll 1$, the atom is elongated with $L_z \gg L_\perp$. We can estimate the longitudinal size L_z by minimizing the energy, $E \sim L_z^{-2} - ZL_z^{-1} \ln(L_z/L_\perp)$ (where the first term is the kinetic energy and the second term is the Coulomb energy), giving

$$L_z \sim \left(Z \ln \frac{1}{Z\rho_m} \right)^{-1}. \quad (2)$$

The energy is given by

$$E_{m0} \sim -Z^2 \left[\ln \frac{1}{Z^2} \left(\frac{b}{2m + 1} \right) \right]^2 \quad (3)$$

for $b \gg (2m + 1)Z^2$. Another type of state of the atom has nodes in the z wave functions ($\nu > 0$). These states are “weakly bound”, and have energies given by $E_{m\nu} \simeq -Z^2 n^{-2}$ Ry, where n is the integer part of $(\nu + 1)/2$. The sizes of the wave functions are ρ_m perpendicular to the field and $L_z \sim \nu^2/Z$ along the field (see Ref. [11] and references therein for more details).

A multielectron atom (with the number of electrons N_e and the charge of the nucleus Z) can be constructed by placing electrons at the lowest available energy levels of a hydrogenic atom. The lowest levels to be filled are the tightly bound states with $\nu = 0$. When $a_0/Z \gg \sqrt{2N_e - 1}\rho_0$, i.e., $b \gg 2Z^2 N_e$, all electrons settle into the tightly bound levels with $m = 0, 1, 2, \dots, N_e - 1$. The energy of the atom is approximately given by the sum of all the eigenvalues of Eq. (3). Accordingly, we obtain an asymptotic expression for $N_e \gg 1$ [52]:

$$E \sim -Z^2 N_e \left(\ln \frac{b}{2Z^2 N_e} \right)^2. \quad (4)$$

For intermediate-strong fields (but still strong enough to ignore Landau excitations), $Z^2 N_e^{-2/3} \ll b \ll 2Z^2 N_e$, many $\nu > 0$ states of the inner Landau orbitals (states with relatively small m) are populated by the electrons. In this regime a Thomas-Fermi type model for the atom is appropriate, i.e., the electrons can be treated as a one-dimensional Fermi gas in a more or less spherical atomic cell (see, e.g., Refs. [53, 54]). The electrons occupy the ground Landau level, with the z momentum up to the Fermi momentum $p_F \sim n/b$, where n is the number density of electrons inside the atom (recall that the degeneracy of a Landau level is $eB/\hbar c \sim b$). The kinetic energy of electrons per unit volume is $\varepsilon_k \sim b p_F^3 \sim n^3/b^2$, and the total kinetic energy is $E_k \sim R^3 n^3/b^2 \sim N_e^3/(b^2 R^6)$, where R is the radius of the atom.

¹ Unless otherwise specified, we use atomic units, in which length is in a_0 (Bohr radius), mass in m_e , energy in $e^2/a_0 = 2$ Ry, and field strength in units of B_0 .

The potential energy is $E_p \sim -ZN_e/R$ (for $N_e \lesssim Z$). Therefore the total energy of the atom can be written as $E \sim N_e^3/(b^2 R^6) - ZN_e/R$. Minimizing E with respect to R yields

$$R \sim (N_e^2/Z)^{1/5} b^{-2/5}, \quad E \sim -(Z^2 N_e)^{3/5} b^{2/5}. \quad (5)$$

For these relations to be valid, the electrons must stay in the ground Landau level; this requires $Z/R \ll \hbar\omega_{Be} = b$, which corresponds to $b \gg Z^2 N_e^{-2/3}$.

B. Molecules

In a strong magnetic field, the mechanism of forming molecules is quite different from the zero-field case [9, 43]. Consider hydrogen as an example. The spin of the electron in a H atom is aligned antiparallel to the magnetic field (flipping the spin would cost $\hbar\omega_{Be}$), therefore two H atoms in their ground states ($m = 0$) do not bind together according to the exclusion principle. Instead, one H atom has to be excited to the $m = 1$ state. The two H atoms, one in the ground state ($m = 0$), another in the $m = 1$ state then form the ground state of the H_2 molecule by covalent bonding. Since the activation energy for exciting an electron in the H atom from the Landau orbital m to $(m+1)$ is small, the resulting H_2 molecule is stable. Similarly, more atoms can be added to form H_3 , H_4 , ... The size of the H_2 molecule is comparable to that of the H atom. The interatomic separation a and the dissociation energy D of the H_2 molecule scale approximately as $a \sim (\ln b)^{-1}$ and $D \sim (\ln b)^2$, although D is numerically smaller than the ionization energy of the H atom.

Consider the molecule Z_N , formed out of N neutral atoms Z (each with Z electrons and nuclear charge Z). For sufficiently large b (see below), the electrons occupy the Landau orbitals with $m = 0, 1, 2, \dots, NZ - 1$, and the transverse size of the molecule is $L_\perp \sim (NZ/b)^{1/2}$. Let a be the atomic spacing and $L_z \sim Na$ the size of the molecule in the z direction. The energy per “atom” in the molecule, $E = E_N/N$, can be written as $E \sim Z(Na)^{-2} - (Z^2/a)l$, where $l \sim \ln(a/L_\perp)$. Variation of E with respect to a gives

$$a \sim (ZN^2 l)^{-1}, \quad E \sim -Z^3 N^2 l^2, \quad \text{with } l \sim \ln\left(\frac{b}{N^5 Z^3}\right). \quad (6)$$

This above scaling behavior is valid for $1 \ll N \ll N_s$. The “critical saturation number” N_s is reached when $a \sim L_\perp$, or when [43]

$$N_s \sim \left(\frac{b}{Z^3}\right)^{1/5}. \quad (7)$$

Beyond N_s , it becomes energetically more favorable for the electrons to settle into the inner Landau orbitals (with smaller m) with nodes in their longitudinal wave functions (i.e., $\nu \neq 0$). For $N \gtrsim N_s$, the energy per atom asymptotes to a value $E \sim -Z^{9/5} b^{2/5}$, and size of the atom scales as $L_\perp \sim a \sim Z^{1/5} b^{-2/5}$, independent of N — the molecule essentially becomes one-dimensional condensed matter.

The scaling relations derived above are obviously crude — they are expected to be valid only in the asymptotic limit, $\ln(b/Z^3) \gg 1$. For realistic neutron stars, this limit is not quite reached. Thus these scaling results should only serve as a guide to the energies of various molecules. For a given field strength, it is not clear from the above analysis whether the Z_N molecule is bound relative to individual atoms. To answer this question requires quantitative calculations.

III. DENSITY-FUNCTIONAL CALCULATIONS: METHODS AND EQUATIONS

Our calculations will be based on the “adiabatic approximation,” in which all electrons are assumed to lie in the ground Landau level. For atoms or molecules with nucleus charge number Z , this is an excellent approximation for $b \gg Z^2$. Even under more relaxed condition, $b \gg Z^{4/3}$ (assuming the number of electrons in each atom is $N_e \sim Z$) this approximation is expected to yield a reasonable total energy of the system and accurate results for the energy difference between different atoms and molecules; a quantitative evaluation of this approximation in this regime is beyond the scope of this paper (but see Refs. [30, 31, 32]).

In the adiabatic approximation, the one-electron wave function (“orbital”) can be separated into a transverse (perpendicular to the external magnetic field) component and a longitudinal (along the magnetic field) component:

$$\Psi_{m\nu}(\mathbf{r}) = W_m(\mathbf{r}_\perp) f_{m\nu}(z). \quad (8)$$

Here W_m is the ground-state Landau wave function [55] given by

$$W_m(\mathbf{r}_\perp) = \frac{1}{\rho_0 \sqrt{2\pi m!}} \left(\frac{\rho}{\sqrt{2}\rho_0} \right)^m \exp \left(\frac{-\rho^2}{4\rho_0^2} \right) \exp(-im\phi), \quad (9)$$

where $\rho_0 = (\hbar c/eB)^{1/2}$ is the cyclotron radius (or magnetic length), and $f_{m\nu}$ is the longitudinal wave function which must be solved numerically. We normalize $f_{m\nu}$ over all space:

$$\int_{-\infty}^{\infty} dz |f_{m\nu}(z)|^2 = 1, \quad (10)$$

so that $\int d\mathbf{r} |\Psi_{m\nu}(\mathbf{r})|^2 = 1$. The density distribution of electrons in the atom or molecule is

$$n(\mathbf{r}) = \sum_{m\nu} |\Psi_{m\nu}(\mathbf{r})|^2 = \sum_{m\nu} |f_{m\nu}(z)|^2 |W_m|^2(\rho), \quad (11)$$

where the sum is over all the electrons in the atom or molecule, with each electron occupying an $(m\nu)$ orbital. The notation $|W_m|^2(\rho) = |W_m(\mathbf{r}_\perp)|^2$ is used here because W_m is a function of ρ and ϕ but $|W_m|^2$ is a function only of ρ .

In an external magnetic field, the Hamiltonian of a free electron is

$$\hat{H} = \frac{1}{2m_e} \left(\mathbf{p} + \frac{e}{c} \mathbf{A} \right)^2 + \frac{\hbar e B}{2m_e c} \sigma_z, \quad (12)$$

where $\mathbf{A} = \frac{1}{2} \mathbf{B} \times \mathbf{r}$ is the vector potential of the external magnetic field and σ_z is the z component Pauli spin matrix. For electrons in Landau levels, with their spins aligned parallel/antiparallel to the magnetic field, the Hamiltonian becomes

$$\hat{H} = \frac{\hat{p}_z^2}{2m_e} + \left(n_L + \frac{1}{2} \right) \hbar \omega_{Be} \pm \frac{1}{2} \hbar \omega_{Be}, \quad (13)$$

where $n_L = 0, 1, 2, \dots$ is the Landau level index; for electrons in the ground Landau level, with their spins aligned antiparallel to the magnetic field (so $n_L = 0$ and $\sigma_z \rightarrow -1$),

$$\hat{H} = \frac{\hat{p}_z^2}{2m_e}. \quad (14)$$

The total Hamiltonian for the atom or molecule then becomes

$$\hat{H} = \sum_i \frac{\hat{p}_{z,i}^2}{2m_e} + V, \quad (15)$$

where the sum is over all electrons and V is the total potential energy of the atom or molecule. From this we can derive the total energy of the system.

Note that we use nonrelativistic quantum mechanics in our calculations, even when $\hbar \omega_{Be} \gtrsim m_e c^2$ or $B \gtrsim B_Q = B_0/\alpha^2 = 4.414 \times 10^{13}$ G. This is valid for two reasons: (i) The free-electron energy in relativistic theory is

$$E = \left[c^2 p_z^2 + m_e^2 c^4 \left(1 + 2n_L \frac{B}{B_Q} \right) \right]^{1/2}. \quad (16)$$

For electrons in the ground Landau level ($n_L = 0$), Eq. (16) reduces to $E \simeq m_e c^2 + p_z^2/(2m_e)$ for $p_z c \ll m_e c^2$; the electron remains nonrelativistic in the z direction as long as the electron energy is much less than $m_e c^2$; (ii) Eq. (9) indicates that the shape of Landau transverse wave function is independent of particle mass, and thus Eq. (9) is valid in the relativistic theory. Our calculations assume that the longitudinal motion of the electron is nonrelativistic. This is valid at all field strengths and for all elements considered with the exception of iron at $B \gtrsim 10^{15}$ G. Even at $B = 2 \times 10^{15}$ G (the highest field considered in this paper), however, we find that the most-bound electron in any Fe atom or molecule has a longitudinal kinetic energy of only $\sim 0.2 m_e c^2$ and only the three most-bound electrons have longitudinal kinetic energies $\gtrsim 0.1 m_e c^2$. Thus relativistic corrections are small in the field strengths considered in this paper. Moreover, we expect our results for the relative energies between Fe atoms and molecules to be much more accurate than the absolute energies of either the atoms or the molecules.

Consider the molecule Z_N , consisting of N atoms, each with an ion of charge Z and Z electrons. In the lowest-energy state of the system, the ions are aligned along the magnetic field. The spacing between ions, a , is chosen to be constant across the molecule. In the density functional theory, the total energy of the system can be represented as a functional of the total electron density $n(\mathbf{r})$:

$$E[n] = E_K[n] + E_{eZ}[n] + E_{\text{dir}}[n] + E_{\text{exc}}[n] + E_{ZZ}[n]. \quad (17)$$

Here $E_K[n]$ is the kinetic energy of a system of noninteracting electrons, and E_{eZ} , E_{dir} , and E_{ZZ} are the electron-ion Coulomb energy, the direct electron-electron interaction energy, and the ion-ion interaction energy, respectively,

$$E_{eZ}[n] = -\sum_{j=1}^N Ze^2 \int d\mathbf{r} \frac{n(\mathbf{r})}{|\mathbf{r} - \mathbf{z}_j|}, \quad (18)$$

$$E_{\text{dir}}[n] = \frac{e^2}{2} \iint d\mathbf{r} d\mathbf{r}' \frac{n(\mathbf{r})n(\mathbf{r}')}{|\mathbf{r} - \mathbf{r}'|}, \quad (19)$$

$$E_{ZZ}[n] = \sum_{j=1}^{N-1} (N-j) \frac{Z^2 e^2}{ja}. \quad (20)$$

The location of the ions in the above equations is represented by the set $\{\mathbf{z}_j\}$, with

$$\mathbf{z}_j = (2j - N - 1) \frac{a}{2} \hat{\mathbf{z}}. \quad (21)$$

The term E_{exc} represents exchange-correlation energy. In the local approximation,

$$E_{\text{exc}}[n] = \int d\mathbf{r} n(\mathbf{r}) \varepsilon_{\text{exc}}(n), \quad (22)$$

where $\varepsilon_{\text{exc}}(n) = \varepsilon_{\text{ex}}(n) + \varepsilon_{\text{corr}}(n)$ is the exchange and correlation energy per electron in a uniform electron gas of density n . For electrons in the ground Landau level, the (Hartree-Fock) exchange energy can be written as follows [56]:

$$\varepsilon_{\text{ex}}(n) = -\pi e^2 \rho_0^2 n F(t), \quad (23)$$

where the dimensionless function $F(t)$ is

$$F(t) = 4 \int_0^\infty dx \left[\tan^{-1} \left(\frac{1}{x} \right) - \frac{x}{2} \ln \left(1 + \frac{1}{x^2} \right) \right] e^{-4tx^2}, \quad (24)$$

and

$$t = \left(\frac{n}{n_B} \right)^2 = 2\pi^4 \rho_0^6 n^2, \quad (25)$$

[$n_B = (\sqrt{2}\pi^2 \rho_0^3)^{-1}$ is the density above which the higher Landau levels start to be filled in a uniform electron gas]. For small t , $F(t)$ can be expanded as follows [57]:

$$F(t) \simeq 3 - \gamma - \ln 4t + \frac{2t}{3} \left(\frac{13}{6} - \gamma - \ln 4t \right) + \frac{8t^2}{15} \left(\frac{67}{30} - \gamma - \ln 4t \right) + \mathcal{O}(t^3 \ln t), \quad (26)$$

where $\gamma = 0.5772 \dots$ is Euler's constant. We have found that the condition $t \ll 1$ is well satisfied everywhere for almost all molecules in our calculations. The notable exceptions are the carbon molecules at $B = 10^{12}$ G and the iron molecules at $B = 10^{13}$ G, which have $t \lesssim 1$ near the center of the molecule. These molecules are expected to have higher t values than the other molecules in our calculations, as they have large Z and low B .²

² For the uniform gas model, $t \propto Z^{6/5} N_e^{-2/5} B^{-3/5}$.

The correlation energy of uniform electron gas in strong magnetic fields has not been calculated in general, except in the regime $t \ll 1$ and Fermi wavenumber $k_F = 2\pi^2 \rho_0^2 n \gg 1$ [or $n \gg (2\pi^3 \rho_0^2 a_0)^{-1}$]. Skudlarski and Vignale [58] use the random-phase approximation to find a numerical fit for the correlation energy in this regime (see also Ref. [59]):

$$\varepsilon_{\text{corr}} = -\frac{e^2}{\rho_0} [0.595(t/b)^{1/8}(1 - 1.009t^{1/8})]. \quad (27)$$

In the absence of an “exact” correlation energy density we employ this strong-field-limit expression. Fortunately, because we are concerned mostly with finding energy changes between different states of atoms and molecules, the correlation energy term does not have to be exact. The presence or the form of the correlation term has a modest effect on the atomic and molecular energies calculated but has very little effect on the energy difference between them (see Appendix B for more details on various forms of the correlation energy and comparisons).

Variation of the total energy with respect to the total electron density, $\delta E[n]/\delta n = 0$, leads to the Kohn-Sham equations:

$$\left[-\frac{\hbar^2}{2m_e} \nabla^2 + V_{\text{eff}}(\mathbf{r}) \right] \Psi_{m\nu}(\mathbf{r}) = \varepsilon_{m\nu} \Psi_{m\nu}(\mathbf{r}), \quad (28)$$

where

$$V_{\text{eff}}(\mathbf{r}) = -\sum_{j=1}^N \frac{Ze^2}{|\mathbf{r} - \mathbf{z}_j|} + e^2 \int d\mathbf{r}' \frac{n(\mathbf{r}')}{|\mathbf{r} - \mathbf{r}'|} + \mu_{\text{exc}}(n), \quad (29)$$

with

$$\mu_{\text{exc}}(n) = \frac{\partial(n\varepsilon_{\text{exc}})}{\partial n}. \quad (30)$$

Averaging the Kohn-Sham equations over the transverse wave function yields a set of one-dimensional equations:

$$\left(-\frac{\hbar^2}{2m_e} \frac{d^2}{dz^2} - \sum_{j=1}^N Ze^2 \int d\mathbf{r}_\perp \frac{|W_m|^2(\rho)}{|\mathbf{r} - \mathbf{z}_j|} + e^2 \iint d\mathbf{r}_\perp d\mathbf{r}' \frac{|W_m|^2(\rho) n(\mathbf{r}')}{|\mathbf{r} - \mathbf{r}'|} \right. \\ \left. + \int d\mathbf{r}_\perp |W_m|^2(\rho) \mu_{\text{exc}}(n) \right) f_{m\nu}(z) = \varepsilon_{m\nu} f_{m\nu}(z). \quad (31)$$

These equations are solved self-consistently to find the eigenvalue $\varepsilon_{m\nu}$ and the longitudinal wave function $f_{m\nu}(z)$ for each orbital occupied by the ZN electrons. Once these are known, the total energy of the system can be calculated using

$$E[n] = \sum_{m\nu} \varepsilon_{m\nu} - \frac{e^2}{2} \iint d\mathbf{r} d\mathbf{r}' \frac{n(\mathbf{r}) n(\mathbf{r}')}{|\mathbf{r} - \mathbf{r}'|} + \int d\mathbf{r} n(\mathbf{r}) [\varepsilon_{\text{exc}}(n) - \mu_{\text{exc}}(n)] + \sum_{j=1}^{N-1} (N-j) \frac{Z^2 e^2}{ja}. \quad (32)$$

Details of our method used in computing the various integrals and solving the above equations are given in Appendix A.

Note that for a given system, the occupations of electrons in different $(m\nu)$ orbitals are not known *a priori*, and must be determined as part of the procedure of finding the minimum energy state of the system. In our calculation, we first guess n_0, n_1, n_2, \dots , the number of electrons in the $\nu = 0, 1, 2, \dots$ orbitals, respectively (e.g., the electrons in the $\nu = 0$ orbitals have $m = 0, 1, 2, \dots, n_0 - 1$). Note that $n_0 + n_1 + n_2 + \dots = NZ$. We find the energy of the system for this particular set of electron occupations. We then vary the electron occupations and repeat the calculation until the true minimum energy state is found. Obviously, in the case of molecules, we must vary the ion spacing a to determine the equilibrium separation and the the ground-state energy of the molecule. Graphical examples of how the ground state is chosen are given in the next section.

IV. RESULTS

In this section we present our results for the parallel configuration of H_N (up to $N = 10$), He_N (up to $N = 8$), C_N (up to $N = 5$), and Fe_N (up to $N = 3$) at various magnetic field strengths between $B = 10^{12}$ G and 2×10^{15} G.

For each molecule (or atom), data is given in tabular form on the molecule's ground-state energy, the equilibrium separation of the ions in the molecule, and its orbital structure (electron occupation numbers n_0, n_1, n_2, \dots). In some cases the first-excited-state energies are given as well, when the ground-state and first-excited-state energies are similar in value. We also provide the ground-state energies for selected ionization states of C and Fe atoms; among other uses, these quantities are needed for determining the ion emission from a condensed neutron star surface [48]. All of the energies presented in this section are calculated to better than 0.1% numerical accuracy (see Appendix A).

For each of the molecules and ions presented in this section we provide numerical scaling relations for the ground-state energy as a function of magnetic field, in the form of a scaling exponent β with $E_N \propto B_{12}^\beta$. We have provided this information to give readers easy access to energy values for fields in between those listed in the tables. The ground-state energy is generally not well fit by a constant β over the entire magnetic field range covered by this work, so we have provided β values over several different magnetic field ranges. Note that the theoretical value $\beta = 2/5$ (see Sec. II) is approached only in certain asymptotic limits.

We discuss here briefly a few trends in the data: All of the molecules listed in the following tables are bound. The Fe_2 and Fe_3 molecules at $B_{12} = 5$ are not bound, so we have not listed them here, but we have listed the Fe atom at this field strength for comparison with other works. All of the bound molecules listed below have ground-state energies per atom that decrease monotonically with increasing N , with the exception of H_N at $B_{12} = 1$, which has a slight upward glitch in energy at H_4 (see Table I). Additionally, these energies approach asymptotic values for large N — the molecule essentially becomes one-dimensional condensed matter [48]. The equilibrium ion separations also approach asymptotic values for large N , but there is no strong trend in the direction of approach: sometimes the equilibrium ion separations increase with increasing N , sometimes they decrease, and sometimes they oscillate back and forth.

In general, we find that for a given molecule (e.g., Fe_3), the number of electrons in $\nu > 0$ states decreases as the magnetic field increases. This is because the characteristic transverse size $\rho_0 \propto B^{-1/2}$ decreases, so the electrons prefer to stay in the $\nu = 0$ states. For a given field strength, as the number of electrons in the system NN_e increases (e.g., from Fe_2 to Fe_3), more electrons start to occupy the $\nu > 0$ states since the average electron-nucleus separation $\rho_m \propto (2m+1)^{1/2}B^{-1/2}$ becomes too large for large m . For large enough N the value of n_0 , the number of electrons in $\nu = 0$ states, levels off, approaching its infinite chain value (see Ref. [48]). Similar trends happen with n_1, n_2 , etc., though much more slowly.

There are two ways that we have checked the validity of our results by comparison with other works. First, we have repeated several of our atomic and molecular calculations using the correlation energy expression empirically determined by Jones [37]:

$$\varepsilon_{\text{corr}} = -\frac{e^2}{\rho_0}(0.0096 \ln \rho_0^3 n + 0.122). \quad (33)$$

The results we then obtain for the atomic ground-state energies agree with those of Jones [37, 38]. For example, for Fe at $B_{12} = 5$ we find an atomic energy of -108.05 eV and Jones gives an energy of -108.18 eV. The molecular ground-state energies per atom are of course not the same as those for the infinite chain from Jones's work, but they are comparable, particularly for the large molecules. For example, we find for He_8 at $B_{12} = 5$ that the energy per atom is -1242 eV and Jones finds for He_∞ that the energy per cell is -1260 eV. (See Appendix B for a brief discussion of why in our calculations we chose to use the Skudlarski-Vignale correlation energy expression over that of Jones.)

Second, we have compared our hydrogen, helium, and carbon molecule results to those of Refs. [43, 47]. Because these works use the Hartree-Fock method, we cannot compare absolute ground-state energies with theirs, but we can compare energy differences. We find fair agreement, though the Hartree-Fock results are consistently smaller. Some of these comparisons are presented in the following subsections.

A. Hydrogen

Our numerical results for H are given in Table I and Table II. Note that at $B_{12} = 1$, H_4 is less bound than H_3 , and thus $E = E_N/N$ is not a necessarily a monotonically decreasing function of N at this field strength. For the H_4 molecule, two configurations, $(n_0, n_1) = (4, 0)$ and $(3, 1)$, have very similar equilibrium energies (see Fig. 1), although the equilibrium ion separations are different. The real ground state may therefore be a “mixture” of the two configurations; such a state would presumably give a lower ground-state energy for H_4 , and make the energy trend monotonic.

Hartree-Fock results for H molecules are given in [43]. For H_2 , H_3 , and H_4 , the energies (per atom) are, respectively: $-184.3, -188.7, -185.0$ eV at $B_{12} = 1$; $-383.9, -418.8, -432.9$ eV at $B_{12} = 10$; and $-729.3, -847.4, -915.0$ eV at

TABLE I: Ground-state energies, ion separations, and electron configurations of hydrogen molecules, over a range of magnetic field strengths. In some cases the first-excited-state energies are also listed. Energies are given in units of eV, separations in units of a_0 (the Bohr radius). For molecules (H_N) the energy per atom is given, $E = E_N/N$. All of the H and H_2 molecules listed here have electrons only in the $\nu = 0$ states. For the H_3 and larger molecules here, however, the molecular structure is more complicated, and is designated by the notation (n_0, n_1, \dots) , where n_0 is the number of electrons in the $\nu = 0$ orbitals, n_1 is the number of electrons in the $\nu = 1$ orbitals, etc.

B_{12}	H		H_2		H_3			H_4			H_5		
	E	a	E	a	E	a	(n_0, n_1)	E	a	(n_0, n_1)	E	a	(n_0, n_1)
1	-161.4		-201.1	0.25	-209.4	0.22	(3,0)	-208.4	0.21	(4,0)	-213.8	0.23	(4,1)
					-191.1	0.34	(2,1)	-207.9	0.26	(3,1)	-203.1	0.200	(5,0)
10	-309.5		-425.8	0.125	-469.0	0.106	(3,0)	-488.1	0.096	(4,0)	-493.5	0.090	(5,0)
											-478.9	0.112	(4,1)
100	-540.3		-829.5	0.071	-961.2	0.057	(3,0)	-1044.5	0.049	(4,0)	-1095.5	0.044	(5,0)
1000	-869.6		-1540.5	0.044	-1818.0	0.033	(3,0)	-2049	0.028	(4,0)	-2222	0.024	(5,0)

B_{12}	H_6			H_8			H_{10}		
	E	a	(n_0, n_1)	E	a	(n_0, n_1, n_2)	E	a	(n_0, n_1, n_2)
1	-214.1	0.23	(4,2)	-215.8	0.23	(5,2,1)	-216.2	0.22	(6,3,1)
	-213.4	0.21	(5,1)	-215.3	0.25	(4,3,1)	-216.0	0.23	(5,3,2)
10	-496.5	0.101	(5,1)	-507.1	0.095	(8,2,0)	-509.3	0.091	(7,3,0)
	-490.8	0.86	(6,0)	-504.1	0.089	(7,1,0)	-506.8	0.087	(8,2,0)
100	-1125.0	0.041	(6,0)	-1143.0	0.038	(8,0,0)	-1169.5	0.038	(9,1,0)
				-1139.5	0.043	(7,1,0)	-1164.0	0.042	(8,2,0)
1000	-2351	0.22	(6,0)	-2518	0.0190	(8,0,0)	-2600	0.0170	(10,0,0)
							-2542	0.0200	(9,1,0)

TABLE II: Fit of the ground-state energies of hydrogen molecules to the scaling relation $E \propto B_{12}^\beta$. The scaling exponent β is fit for each molecule H_N over three magnetic field ranges: $B_{12} = 1 - 10$, $10 - 100$, and $100 - 1000$.

B_{12}	β							
	H	H_2	H_3	H_4	H_5	H_6	H_8	H_{10}
1-10	0.283	0.326	0.350	0.370	0.363	0.365	0.371	0.372
10-100	0.242	0.290	0.312	0.330	0.346	0.355	0.353	0.361
100-1000	0.207	0.269	0.277	0.293	0.307	0.320	0.343	0.347

$B_{12} = 100$. Thus, our density-functional-theory calculation tends to overestimate the energy $|E|$ by about 10%. Note that the Hartree-Fock results also reveal a non-monotonic behavior of E at $N = 4$ for $B_{12} = 1$, in agreement with our density-functional result. Demeur *et al.* [47] calculated the energies of H_2 – H_5 at $B_{12} = 2.35$; their results exhibit similar trends.

B. Helium

Our numerical results for He are given in Table III and Table IV.

The energies (per atom) of He and He_2 based on Hartree-Fock calculations [11] are, respectively: -575.5 , -601.2 eV at $B_{12} = 1$; -1178 , -1364 eV at $B_{12} = 10$; -2193 , -2799 eV at $B_{12} = 100$; and -3742 , -5021 eV at $B_{12} = 1000$. At $B_{12} = 2.35$, Demeur *et al.* [47] find that the energies (per atom) of He, He_2 , He_3 , and He_4 are, respectively: -753.4 , -812.6 , -796.1 , -805.1 eV. Using our scaling relations, we find for that same field that the energies of He, He_2 , He_3 , and He_5 (we do not have an He_4 result) are: -791 , -871 , -889 , -901 eV. Thus, our density-functional theory calculation tends to overestimate the energy $|E|$ by about 10%.

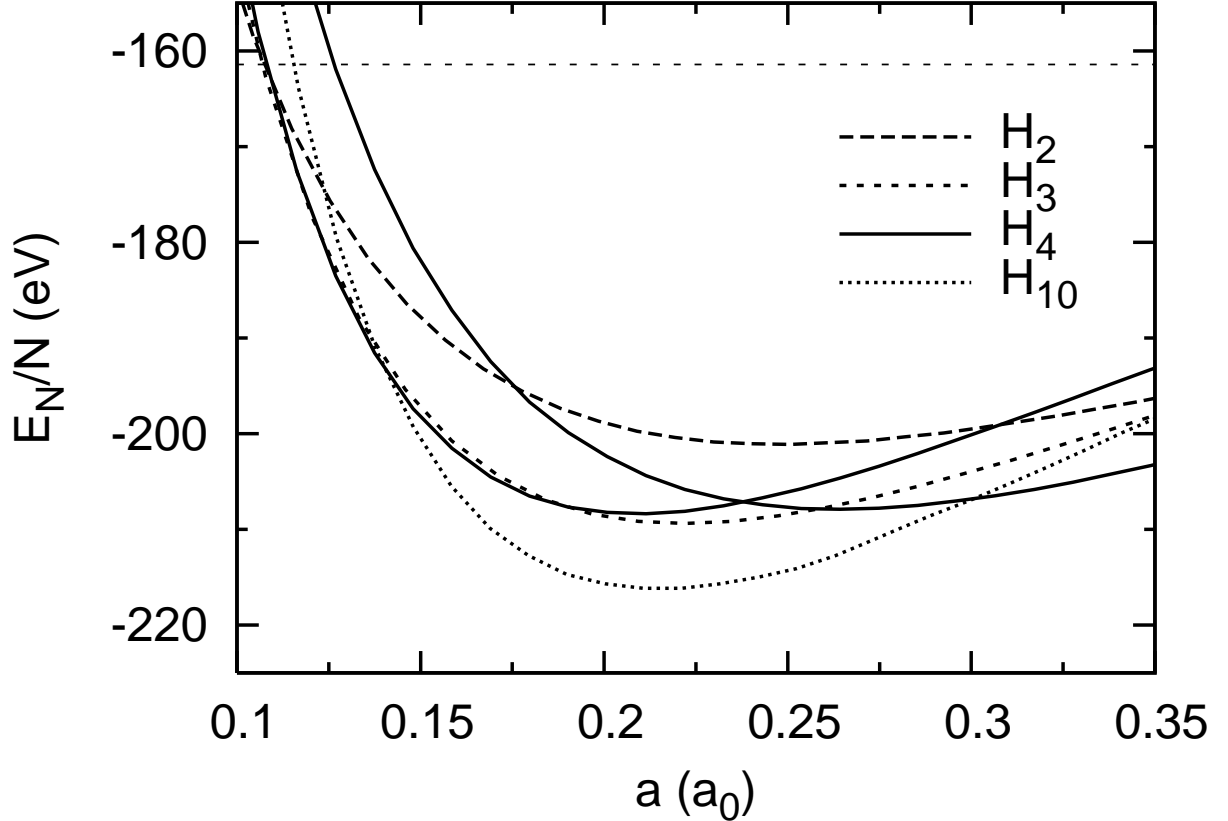


FIG. 1: Molecular energy per atom versus ion separation for various hydrogen molecules at $B_{12} = 1$. The energy of the H atom is shown as a horizontal line at -161.4 eV. The two lowest-energy configurations of H_4 have nearly the same minimum energy, so the curves for both configurations are shown here.

C. Carbon

Our numerical results for C are given in Table V, Table VI, and Table VII.

The only previous result of C molecules is that by Demeur *et al.* [47], who calculated C_2 only at $B_{12} = 2.35$. At this field strength, our calculation shows that C_2 is bound relative to C atom ($E = -5994, -6017$ eV for C, C_2), whereas Demeur *et al.* find no binding ($E = -5770, -5749$ eV for C, C_2). Thus our result differs qualitatively from [47]. We also disagree on the ground-state occupation at this field strength: we find $(n_0, n_1) = (9, 3)$ while Demeur *et al.* find $(n_0, n_1) = (7, 5)$. We suggest that if Demeur *et al.* used the occupation $(n_0, n_1) = (9, 3)$ they would obtain a lower-energy for C_2 , though whether C_2 would then be bound remains uncertain. Since the numerical accuracy of our computation is 0.1% of the total energy (thus, about 6 eV for $B_{12} = 2.35$), our results for $B_{12} \lesssim$ a few should be treated with caution.

Figure 2 gives some examples of the longitudinal electron wave functions. One wave function of each node type in the molecule ($\nu = 0$ to 4) is represented. Note that on the atomic scale each wave function is nodeless in nature; that is, there are no nodes at the ions, only in between ions. The exception to this is at the central ion, where due to symmetry considerations the antisymmetric wave functions must have nodes. [The nodes for $(m, \nu) = (0, 2)$ are near, but not at, the ions $j = 2$ and $j = 4$. This is incidental.] This is not surprising when one considers that all of the electrons in atomic carbon at this field strength are nodeless. The entire molecular wave function can be thought of as a string of atomic wave functions, one around each ion, each modified by some phase factor to give the overall nodal nature of the wave function. Indeed, for atoms at field strengths that are low enough to allow $\nu > 0$ states, we find that their corresponding molecules have electron wave functions with nodes at the ions. Atomic Fe at $B_{12} = 10$, for example, has an electron wave function with one node at the ion, and Fe_2 at $B_{12} = 10$ has an electron wave function with a node at each ion.

TABLE III: Ground-state energies, ion separations, and electron configurations of helium molecules, over a range of magnetic field strengths. In some cases the first-excited-state energies are also listed. Energies are given in units of eV, separations in units of a_0 (the Bohr radius). For molecules (He_N) the energy per atom is given, $E = E_N/N$. All of the He and He_2 molecules listed here have electrons only in the $\nu = 0$ states. For the He_3 and larger molecules here, however, the molecular structure is more complicated, and is designated by the notation (n_0, n_1, \dots) , where n_0 is the number of electrons in the $\nu = 0$ orbitals, n_1 is the number of electrons in the $\nu = 1$ orbitals, etc.

B_{12}	He	He_2		He_3			He_5			He_8		
	E	E	a	E	a	(n_0, n_1)	E	a	(n_0, n_1, n_2)	E	a	(n_0, n_1, n_2, n_3)
1	-603.5	-641.2 0.25		-647.3 0.28	(5,1)		-653.1 0.29	(6,3,1)		-656.7 0.28	(7,5,3,1)	
				-633.0 0.32	(4,2)		-649.4 0.28	(7,2,1)		-656.5 0.27	(8,5,2,1)	
10	-1252.0	-1462.0 0.115		-1520.0 0.105	(6,0)		-1553.5 0.110	(8,2,0)		-1574.5 0.110	(10,5,1,0)	
				-1462.0 0.125	(5,1)		-1547.5 0.105	(9,1,0)		-1574.0 0.105	(11,4,1,0)	
100	-2385	-3039 0.060		-3370 0.050	(6,0)		-3573 0.044	(10,0,0)		-3694 0.045	(13,3,0,0)	
				-3140 0.054	(5,1)		-3543 0.049	(9,1,0)		-3690 0.043	(14,2,0,0)	
1000	-4222	-5787 0.036		-6803 0.028	(6,0)		-7887 0.022	(10,0,0)		-8406 0.0200	(15,1,0,0)	
										-8357 0.0180	(16,0,0,0)	

TABLE IV: Fit of the ground-state energies of helium molecules to the scaling relation $E \propto B_{12}^\beta$. The scaling exponent β is fit for each molecule He_N over three magnetic field ranges: $B_{12} = 1 - 10$, $10 - 100$, and $100 - 1000$.

B_{12}	β				
	He	He_2	He_3	He_5	He_8
1-10	0.317	0.358	0.371	0.376	0.380
10-100	0.280	0.318	0.346	0.362	0.370
100-1000	0.248	0.280	0.305	0.344	0.357

D. Iron

Our numerical results for Fe are given in Table VIII, Table IX, and Table X. The energy curves for $B_{12} = 500$ are shown in Fig. 3, and some results for $B_{12} = 100$ are shown in Fig. 4.

There is no previous quantitative calculation of Fe molecules in strong magnetic fields that we are aware of. The most relevant work is that of Abrahams and Shapiro [60], who use a Thomas-Fermi type model to calculate Fe and Fe_2 energies for magnetic fields up to $B_{12} = 30$. Unfortunately, a comparison of our results with those of this work is not very useful, as Thomas-Fermi models are known to give inaccurate energies and in particular large overestimates

TABLE V: Ground-state energies, ion separations, and electron configurations of carbon molecules, over a range of magnetic field strengths. In some cases the first-excited-state energies are also listed. Energies are given in units of eV, separations in units of a_0 (the Bohr radius). For molecules (C_N) the energy per atom is given, $E = E_N/N$. All of the C atoms listed here have electrons only in the $\nu = 0$ orbitals. For the C_2 and larger molecules here, however, the molecular structure is more complicated, and is designated by the notation (n_0, n_1, \dots) , where n_0 is the number of electrons in the $\nu = 0$ orbitals, n_1 is the number of electrons in the $\nu = 1$ orbitals, etc.

B_{12}	C	C_2			C_3			C_4			C_5		
	E	E	a	(n_0, n_1)	E	a	(n_0, n_1, n_2)	E	a	(n_0, n_1, n_2, n_3)	E	a	$(n_0, n_1, n_2, n_3, n_4)$
1	-4341	-4351 0.53		(8,4)	-4356 0.52	(9,6,3)		-4356 0.52	(10,7,4,3)		-4358 0.48	(11,8,6,3,2)	
		-4349	0.46	(9,3)	-4354 0.50	(10,5,3)		-4354 0.56	(9,7,5,3)		-4357 0.47	(12,8,5,3,2)	
10	-10075	-10215 0.150		(11,1)	-10255 0.175	(13,4,1)		-10255 0.180	(15,6,2,1)		-10275 0.150	(18,8,3,1)	
		-10200	0.180	(10,2)	-10240 0.185	(14,3,1)		-10250 0.185	(14,7,2,1)		-10270 0.155	(17,9,3,1)	
100	-21360	-23550 0.054		(12,0)	-24060 0.055	(17,1,0)		-24350 0.054	(21,3,0,0)		-24470 0.057	(23,6,1,0,0)	
					-23960 0.058	(16,2,0)		-24300 0.056	(20,4,0,0)		-24460 0.056	(24,5,1,0,0)	
1000	-41330	-50760 0.027		(12,0)	-54870 0.024	(18,0,0)		-56500 0.024	(23,1,0,0)		-57640 0.022	(28,2,0,0,0)	
								-56190 0.022	(24,0,0,0)		-57520 0.023	(27,3,0,0,0)	

TABLE VI: Ground-state energies of ionized carbon atoms over a range of magnetic field strengths. Energies are given in units of eV. For these field strengths, the electron configuration of C atoms is such that all of their electrons lie in the $\nu = 0$ orbitals; therefore the ionized atoms have all electrons in the $\nu = 0$ orbitals as well. The ionization state is designated by the notation, “C $^{n+}$,” where n is the number of electrons that have been removed from the atom. The entry “C $^{5+}$,” for example, is a carbon nucleus plus one electron.

B_{12}	C	C $^+$	C $^{2+}$	C $^{3+}$	C $^{4+}$	C $^{5+}$
1	-4341	-4167	-3868	-3411	-2739	-1738.0
10	-10075	-9644	-8917	-7814	-6213	-3877
100	-21360	-20370	-18730	-16300	-12815	-7851
1000	-41330	-39210	-35830	-30920	-24040	-14425

TABLE VII: Fit of the ground-state energies of neutral and ionized carbon atoms and carbon molecules to the scaling relation $E \propto B_{12}^\beta$. The scaling exponent β is fit over three magnetic field ranges: $B_{12} = 1 - 10$, $10 - 100$, and $100 - 1000$.

B_{12}	β							
	C $^{5+}$	C $^{4+}$	C $^+$	C	C $_2$	C $_3$	C $_4$	C $_5$
1-10	0.348	0.356	0.364	0.366	0.371	0.372	0.372	0.372
10-100	0.306	0.314	0.325	0.326	0.363	0.370	0.376	0.377
100-1000	0.264	0.273	0.284	0.287	0.334	0.358	0.366	0.372

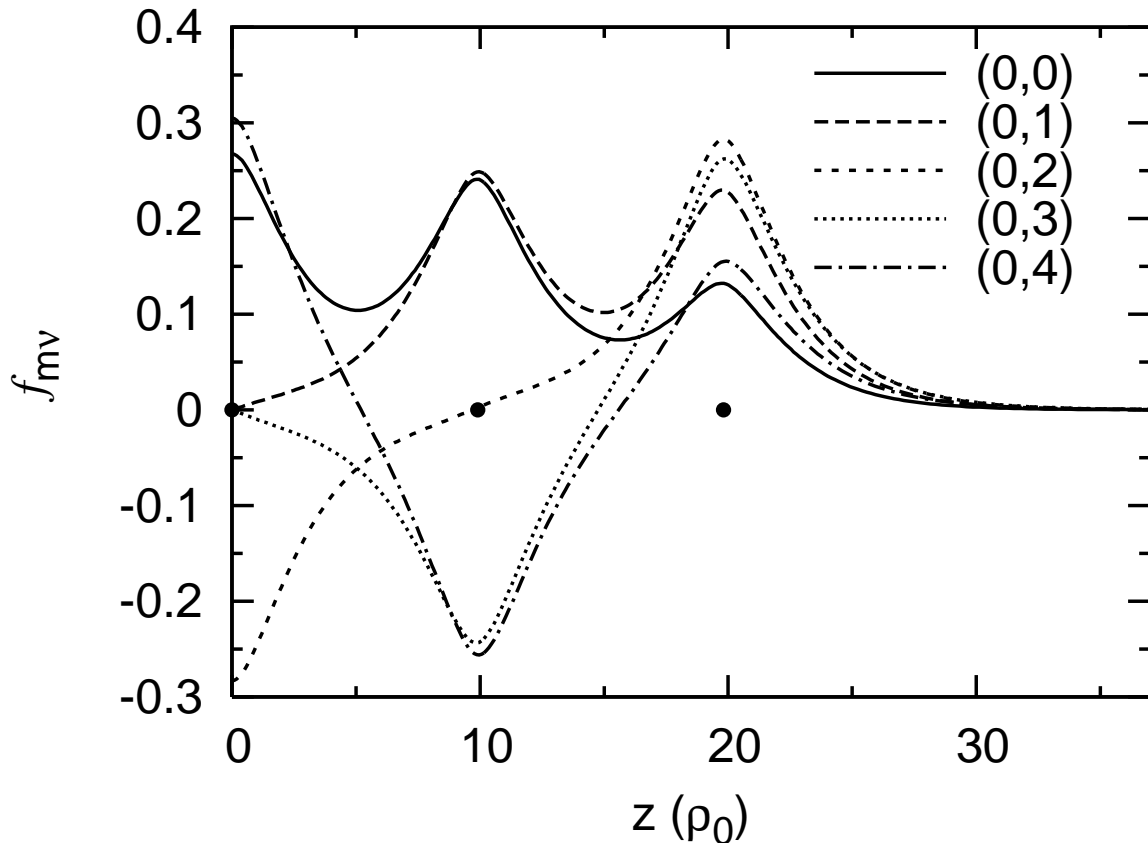


FIG. 2: Longitudinal wave functions for selected electron orbitals of C₅ at $B_{12} = 1$, at the equilibrium ion separation. Different orbitals are labeled by (m, ν) . Only the $z \geq 0$ region is shown. Wave Functions with even ν are symmetric about $z = 0$, and those with odd ν are antisymmetric about $z = 0$. The filled circles denote the ion locations.

TABLE VIII: Ground-state energies, ion separations, and electron configurations of iron molecules, over a range of magnetic field strengths. In some cases the first-excited-state energies are also listed. Energies are given in units of keV, separations in units of a_0 (the Bohr radius). For molecules (Fe_N) the energy per atom is given, $E = E_N/N$. The electron configuration is designated by the notation (n_0, n_1, \dots) , where n_0 is the number of electrons in the $\nu = 0$ orbitals, n_1 is the number of electrons in the $\nu = 1$ orbitals, etc. Note that no information is listed for the Fe_2 and Fe_3 molecules at $B_{12} = 5$, as we have found that these molecules are not bound at this field strength. Also note that there are two lowest-energy states for Fe_2 at $B_{12} = 100$; within the error of our calculation, the two states have the same minimum energies.

B_{12}	Fe		Fe_2			Fe_3		
	E	(n_0, n_1)	E	a	(n_0, n_1)	E	a	(n_0, n_1, n_2)
5	-107.20	(24,2)	-	-	-	-	-	-
10	-142.15	(25,1)	-142.18	0.30	(32,19,1)	-	-	-
100	-354.0	(26,0)	-354.9	0.107	(39,13)	-355.2	0.107	(47,21,10)
			-354.9	0.103	(40,12)	-355.1	0.108	(46,22,10)
500	-637.8	(26,0)	-645.7	0.048	(45,7)	-648.1	0.048	(58,16,4)
			-645.4	0.050	(44,8)	-648.0	0.050	(57,16,5)
1000	-810.6	(26,0)	-828.8	0.035	(47,5)	-834.1	0.035	(62,13,3)
			-828.4	0.034	(48,4)	-834.0	0.036	(61,14,3)
2000	-1021.5	(26,0)	-1061.0	0.025	(49,3)	-1073.0	0.025	(67,10,1)
			-1056.0	0.023	(50,2)	-1072.5	0.025	(66,11,1)

TABLE IX: Ground-state energies of ionized iron atoms over a range of magnetic field strengths. Energies are given in units of keV. For $B_{12} \geq 100$, the electron configuration of Fe atoms is such that all of their electrons lie in the $\nu = 0$ orbitals; therefore for these field strengths the ionized atoms have all electrons in the $\nu = 0$ orbitals as well. The ionization state is designated by the notation, “ Fe^{n+} ,” where n is the number of electrons that have been removed from the atom. The entry “ Fe^{25+} ,” for example, is an iron nucleus plus one electron.

B_{12}	Fe	Fe^+	Fe^{2+}	Fe^{3+}	Fe^{4+}	Fe^{5+}	Fe^{10+}	Fe^{15+}	Fe^{20+}	Fe^{25+}
100	-354.0	-352.8	-351.2	-349.0	-346.4	-343.2	-318.3	-273.8	-199.65	-59.01
500	-637.8	-635.3	-632.0	-627.8	-622.7	-616.6	-569.4	-486.5	-350.2	-99.48
1000	-810.6	-807.2	-802.8	-797.2	-790.7	-782.5	-715.8	-602.0	-439.6	-122.70
2000	-1021.5	-1016.0	-1008.5	-999.8	-989.1	-976.7	-905.4	-768.6	-546.8	-150.10

of binding and cohesive energies. As an example, from Ref. [60] the energy difference between Fe and Fe_2 at $B_{12} = 30$ is 1.7 keV, which is twice as large as our result at $B_{12} = 100$.

In Table VIII we have not provided results for the Fe_2 and Fe_3 molecules at $B_{12} = 5$, as these molecules are not bound relative to the Fe atom. We have not provided results for the Fe_3 molecule at $B_{12} = 10$ because the energy difference (per atom) between Fe_3 and the Fe atom at this field strength is smaller than the error in our calculation, 0.1% of $|E|$ or 140 eV. The energy difference (per atom) between the Fe_2 molecule and the Fe atom at $B_{12} = 10$ is also smaller than the error in our calculation (indeed, the difference should be less than that between Fe_3 and Fe at this field strength), but we have redone the calculation using more grid and integration points such that the energy values reported here for these two molecules are accurate numerically to 0.01% (see Appendix A). At this accuracy, our results indicate that Fe_2 is bound over Fe at $B_{12} = 10$ with a energy difference per atom of 30 eV.

Figure 4 illustrates how the ground-state electron configuration is found for each molecule. The configuration with the lowest equilibrium energy is chosen as the ground-state configuration. In the case depicted in Fig. 4, Fe_2 at $B_{12} = 100$, there are actually two such configurations. Within the error of our calculation, we cannot say which one represents the ground state. Note that the systematic error seen in the minimization curves of the various Fe_2 configurations is much smaller than our target 0.1% error for the total energy (the sinusoidal error in the figure has an amplitude of ≈ 30 eV, or around 0.01% of the total energy).

V. CONCLUSIONS

We have presented density-functional-theory calculations of the ground-state energies of various atoms and molecular chains (H_N up to $N = 10$, He_N up to $N = 8$, C_N up to $N = 5$, and Fe_N up to $N = 3$) in strong magnetic fields ranging

TABLE X: Fit of the ground-state energies of neutral and ionized iron atoms and iron molecules to the scaling relation $E \propto B_{12}^\beta$. The scaling exponent β is fit over three magnetic field ranges: $B_{12} = 100 - 500$, $500 - 1000$, and $1000 - 2000$.

B_{12}					β		
	Fe^{25+}	Fe^{20+}	Fe^{10+}	Fe^+	Fe	Fe_2	Fe_3
100-500	0.324	0.349	0.361	0.365	0.366	0.372	0.374
500-1000	0.303	0.328	0.330	0.345	0.346	0.359	0.364
1000-2000	0.291	0.315	0.339	0.332	0.334	0.358	0.363

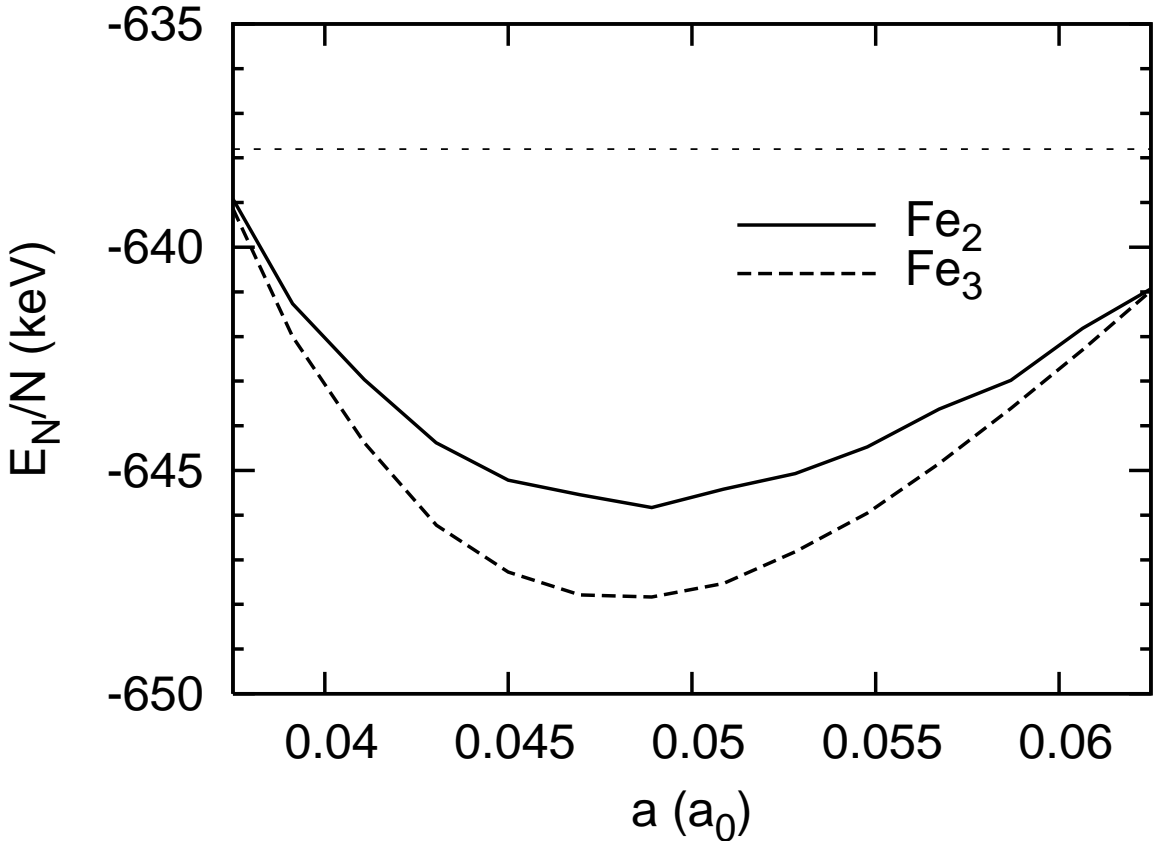


FIG. 3: Molecular energy per atom versus ion separation for Fe_2 and Fe_3 molecules at $B_{12} = 500$. The energy of the Fe atom is shown as a horizontal line at -637.8 keV.

from $B = 10^{12}$ G to 2×10^{15} G. These atoms and molecules may be present in the surface layers of magnetized neutron stars, such as radio pulsars and magnetars. While previous results (based on Hartree-Fock or density-functional-theory calculations) are available for some small molecules at selected field strengths (e.g., Refs. [11, 43, 47]) many other systems (e.g., larger C molecules and Fe molecules) are also computed in this paper. We have made an effort to present our numerical results systematically, including fitting formulae for the B -dependence of the energies. Comparison with previous results (when available) show that our density-functional calculations tend to overestimate the binding energy $|E_N|$ by about 10%. Since it is advantageous to use the density functional theory to study systems containing large number of electrons (e.g., condensed matter; see Ref. [48]), it would be useful to find ways to improve upon this accuracy.

At $B_{12} \geq 1$, hydrogen, helium, and carbon molecules are all more energetically favorable than their atomic counterparts (although for carbon, the relative binding between the atom and molecule is rather small), but iron is not. Iron molecules start to become bound at $B_{12} \gtrsim 10$, and are not decidedly more favorable than isolated atoms until about $B_{12} = 100$.

For the bound molecules considered here, the ground-state energy per atom approaches an asymptotic value as N gets large. The molecule then essentially becomes a one-dimensional infinite chain. We will study such condensed

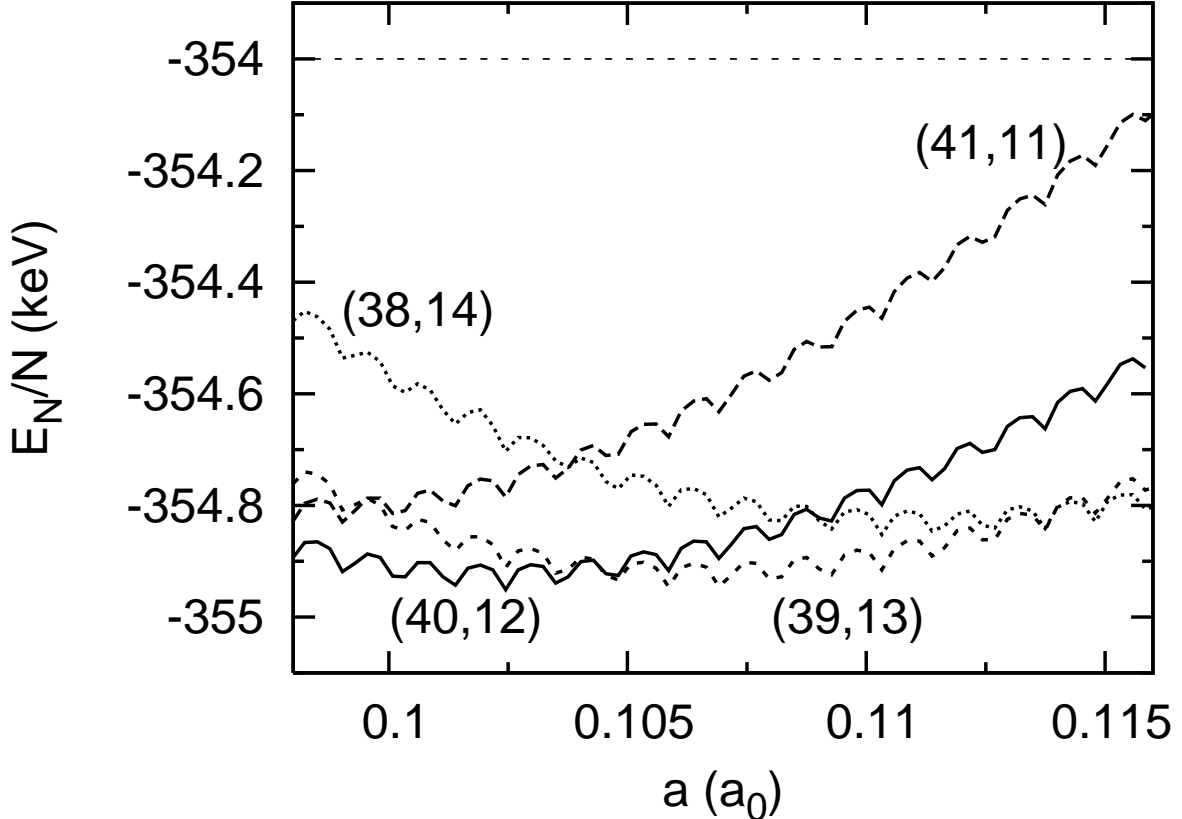


FIG. 4: Molecular energy per atom versus ion separation for various configurations of electrons in the Fe_2 molecule at $B_{12} = 100$. The configurations are labeled using the notation (n_0, n_1) , where n_0 is the number of electrons with $\nu = 0$ and n_1 is the number with $\nu = 1$. The energy of the Fe atom is shown as a horizontal line at -354.0 keV. The states “ $(40, 12)$ ” and “ $(39, 13)$ ” have the lowest equilibrium energies of all possible configurations and within the numerical accuracy of our calculation have the same equilibrium energies. The wavy structure of the curves gives an indication of the numerical accuracy of our code. Note that states with electrons in the $\nu = 2$ orbitals [for example, $(39, 12, 1)$] have energies higher than the atomic energy and are therefore unbound.

matter in our companion paper [48].

Acknowledgments

We thank Neil Ashcroft for useful discussion. This work has been supported in part by NSF Grant No. AST 0307252, NASA Grant No. NAG 5-12034 and *Chandra* Grant No. TM6-7004X (Smithsonian Astrophysical Observatory).

APPENDIX A: NUMERICAL METHOD

1. Evaluating the integrals in the Kohn-Sham equations

The two most computation-intensive terms in the Kohn-Sham equations [Eq. (31)] are the ion-electron interaction term and the direct electron-electron interaction term:

$$V_{Ze,m}(z) = \int d\mathbf{r}_\perp \frac{|W_m|^2(\rho)}{|\mathbf{r} - \mathbf{z}_j|} \quad (\text{A1})$$

and

$$V_{ee,m}(z) = \iint d\mathbf{r}_\perp d\mathbf{r}' \frac{|W_m|^2(\rho) n(\mathbf{r}')}{|\mathbf{r} - \mathbf{r}'|}. \quad (\text{A2})$$

Equation (A1), together with the exchange-correlation term, $\int d\mathbf{r}_\perp |W_m|^2(\rho) \mu_{\text{exc}}(n)$, can be integrated by a standard quadrature algorithm, such as Romberg integration [61]. Equation (A2), however, is more complicated and its evaluation is the rate-limiting step in the entire energy calculation. The integral is over four variables (ρ , ρ' , z' , and ϕ or $\phi - \phi'$), so it requires some simplification to become tractable. To simplify the integral we use the identity (see, e.g., Ref. [62])

$$\frac{1}{|\mathbf{r} - \mathbf{r}'|} = \sum_{n=-\infty}^{\infty} \int_0^{\infty} dq e^{in(\phi - \phi')} J_n(q\rho) J_n(q\rho') e^{-q|z - z'|}, \quad (\text{A3})$$

where $J_n(z)$ is the n th order Bessel function of the first kind. Then

$$\begin{aligned} V_{ee}(\mathbf{r}) &= \int d\mathbf{r}' \frac{n(\mathbf{r}')}{|\mathbf{r} - \mathbf{r}'|} \\ &= 2\pi \int_{-\infty}^{\infty} dz' \int_0^{\infty} dq J_0(q\rho) \left[\int_0^{\infty} \rho' d\rho' n(\rho', z') J_0(q\rho') \right] \exp(-q|z - z'|), \end{aligned} \quad (\text{A4})$$

and

$$\begin{aligned} V_{ee,m}(z) &= \int d\mathbf{r}_\perp |W_m|^2(\rho) V_{ee}(\mathbf{r}) \\ &= 4\pi^2 \int_{-\infty}^{\infty} dz' \int_0^{\infty} dq \left[\int_0^{\infty} \rho d\rho |W_m|^2(\rho) J_0(q\rho) \right] \left[\int_0^{\infty} \rho' d\rho' n(\rho', z') J_0(q\rho') \right] \exp(-q|z - z'|). \end{aligned} \quad (\text{A5})$$

Using Eq. (11) for the electron density distribution, Eq. (A5) becomes

$$V_{ee,m}(z) = \sum_{m'\nu'} \int_{-\infty}^{\infty} dz' |f_{m'\nu'}(z')|^2 \int_0^{\infty} dq G_m(q) G_{m'}(q) \exp(-q|z - z'|), \quad (\text{A6})$$

where

$$\begin{aligned} G_m(q) &= 2\pi \int_0^{\infty} \rho d\rho |W_m|^2(\rho) J_0(q\rho) \\ &= \exp(-q^2/2) L_m(q^2/2), \end{aligned} \quad (\text{A7})$$

and

$$L_m(x) = \frac{e^x}{m!} \frac{d^m}{dx^m} (x^m e^{-x}) \quad (\text{A8})$$

is the Laguerre polynomial of order m . These polynomials can be calculated using the recurrence relation

$$m L_m(x) = (2m - 1 - x) L_{m-1}(x) - (m - 1) L_{m-2}(x), \quad (\text{A9})$$

with $L_0(x) = 1$ and $L_1(x) = 1 - x$.

Using the method outlined above the original four-dimensional integral in Eq. (A2) reduces to a two-dimensional integral. Once a value for z is specified, the integral can be evaluated using a quadrature algorithm (such as the Romberg integration method).

2. Solving the differential equations and total energy

The Kohn-Sham equations [Eq. (31)] are solved on a grid in z . Because of symmetry we only need to consider $z \geq 0$, with $z = 0$ at the center of the molecule. The number and spacing of the z grid points determine how

accurately the equations can be solved. In this paper we have attempted to calculate ground-state energies to better than 0.1% numerical accuracy. This requires approximately (depending on Z and B) 133 grid points for a single atom calculation, plus 66 more for each additional atom in the molecule, or a total of $\approx 66 * (N + 1)$ points for an N -atom molecule. The grid spacing is chosen to be constant from the center out to the outermost ion, then exponentially increasing as the potential decays to zero. The maximum z value for the grid is chosen such that the amplitude of all of the electron wave functions $f_{m\nu}$ at that point is less than 5×10^{-3} .

For integration with respect to ρ , ρ' , or q (e.g., when calculating the direct electron-electron interaction term), our 0.1%-accuracy goal for the energy values requires an accuracy of approximately 10^{-5} in the integral. A variable-step-size integration routine is used for each such integral, where the number of points in the integration grid is increased until the error in the integration is within the desired accuracy.

Solving the Kohn-Sham equations requires two boundary conditions for each $(m\nu)$ orbital. The first is that $f_{m\nu}(z)$ vanishes exponentially for large z . Because the $f_{m\nu}(z)$ wave functions must be symmetric or anti-symmetric about the center of the molecule, there is a second boundary condition: wave functions with an even number of nodes have an extremum at the center and wave functions with an odd number of nodes have a node at the center; i.e., $f'_{m\nu}(0) = 0$ for even ν and $f_{m\nu}(0) = 0$ for odd ν . In practice, we integrate Eq. (31) from the large- z edge of the z grid and “shoot” toward $z = 0$, adjusting $\varepsilon_{m\nu}$ until the boundary condition at the center is satisfied. One final step must be taken to ensure that we have obtained the desired energy and wave function shape, which is to count the number of nodes in the wave function. For each $(m\nu)$ orbital there is only one wave function shape that satisfies the required boundary conditions and has the correct number of nodes ν (e.g., the shape of each orbital in Fig. 2, however complicated-looking, is uniquely determined).

To determine the electronic structure of an atom or molecule self-consistently, a trial set of wave functions is first used to calculate the potential as a function of z , and that potential is used to calculate a new set of wave functions. These new wave functions are then used to find a new potential, and the process is repeated until consistency is reached. In practice, we find that $f_{m\nu}(z) = 0$ works well as the trial wave function, and rapid convergence can be achieved: four or five iterations for atoms and no more than 20 iterations for the largest and most complex molecules. To prevent overcorrection from one iteration to the next, the actual potential used for each iteration is a combination of the newly-generated potential and the old potential from the previous iteration (the weighting used is roughly 30% old, 70% new).

APPENDIX B: CORRELATION ENERGY

As was mentioned in Sec. III, the form of the correlation energy has very little effect on the relative energy between atom and molecule (or between different states of the same molecule). This holds true even if the calculations are done in the extreme case where the correlation energy term is set to zero. As an example, consider the energy of the C_2 molecule at $B = 10^{15}$ G. Using the correlation energy of Skudlarski and Vignale [Eq. (27)], we find the C atom has energy $E_a = -41\,330$ eV and the C_2 molecule has energy per atom $E_m = -50\,760$ eV, so that the relative energy is $\Delta E = 9430$ eV. Using the correlation energy of Jones [Eq. (33)], we find $E_a = -44\,420$ eV and $E_m = -53\,840$ eV, so that $\Delta E = 9420$ eV. Without any correlation term at all, $E_a = -38\,600$ eV and $E_m = -47\,960$ eV, so that $\Delta E = 9360$ eV. As another example of the relative unimportance of the correlation term, two other works using density-functional calculations, Jones [37], Relovsky and Ruder [40], find very similar cohesive energy (i.e., infinite chain) results even though they use two very different correlation energy terms. For example, at $B = 5 \times 10^{12}$ G they both find a cohesive energy of 220 eV for He_∞ .

We make one final comment about the accuracy of our chosen correlation energy term, the Skudlarski-Vignale expression Eq. (27). Jones [37] found an empirical expression for the correlation energy at high B [Eq. (33)], and then checked its accuracy using the fact that the self-interaction of an occupied, self-consistent orbital should be zero, i.e.,

$$E_{\text{dir}}[n_{m\nu}] + E_{\text{exc}}[n_{m\nu}] = 0, \quad (\text{B1})$$

where $n_{m\nu} = |\Psi_{m\nu}(\mathbf{r})|^2$ is the number density of electrons in the $(m\nu)$ orbital. Performing such a test on the Skudlarski-Vignale expression, we find that the error in Eq. (B1) is of order 5–20% for $B_{12} = 1$ and up to 20–30% for $B_{12} = 1000$ for the elements and molecules considered here. Testing Jones’s expression, we find it does as well and sometimes better at $B_{12} = 1$, but at large fields it does considerably worse, up to 60–100% error for $B_{12} = 1000$. For example, for He_2 at $B_{12} = 1000$ the Skudlarski-Vignale correlation function satisfies Eq. (B1) to within 23% but Jones’s expression satisfies Eq. (B1) only to within 63%. Thus, the Skudlarski-Vignale correlation function adopted

in this paper is much more accurate than Jones's expression for a wide range of field strengths.

[1] P. Mészáros, *High-Energy Radiation From Magnetized Neutron Stars* (University of Chicago, Chicago, 1992).

[2] A. Reisenegger, J. P. Prieto, R. Benguria, D. Lai, and P. A. Araya, in *Magnetic Fields in the Universe*, edited by E. M. de Gouveia Dal Pino, G. Lugones, and A. Lazarian, AIP Conf. Proc. No. 784 (AIP, Melville, NY, 2005), p. 263.

[3] A. K. Harding and D. Lai, *Rep. Prog. Phys.* **69**, 2631 (2006).

[4] P. M. Woods and C. Thompson, in *Compact Stellar X-ray Sources*, edited by W. H. G. Lewin and M. van der Klis (Cambridge University, Cambridge, 2005); e-print astro-ph/0406133.

[5] R. C. Duncan and C. Thompson, *Astrophys. J.* **392**, L9 (1992).

[6] C. Thompson and R. C. Duncan, *Mon. Not. R. Astron. Soc.* **275**, 255 (1995).

[7] C. Thompson and R. C. Duncan, *Astrophys. J.* **473**, 332 (1996).

[8] U. Wagner *et al.*, *Phys. Rev. E* **70**, 026401 (2004).

[9] M. Ruderman, in *Physics of Dense Matter*, Proceedings of IAU Symposium No. 53, Boulder, Colorado, edited by C. J. Hansen (Reidel, Dordrecht, 1974), p.117.

[10] H. Ruder, G. Wunner, H. Herold, and F. Geyer, *Atoms in Strong Magnetic Fields* (Springer-Verlag, Berlin, 1994).

[11] D. Lai, *Rev. Mod. Phys.* **73**, 629 (2001).

[12] M. Ruderman and P. G. Sutherland, *Astrophys. J.* **196**, 51 (1975).

[13] J. Arons and E. T. Scharlemann, *Astrophys. J.* **231**, 854 (1979).

[14] V. V. Usov and D. B. Melrose, *Astrophys. J.* **464**, 306 (1996).

[15] A. K. Harding and A. G.Muslimov, *Astrophys. J.* **508**, 328 (1998).

[16] A. M. Beloborodov and C. Thompson, *Astrophys. J.* ; e-print astro-ph/0602417.

[17] D. G. Yakovlev and C. J. Pethick, *Ann. Rev. Astron. Astrophys.* **42**, 169 (2004).

[18] V. M. Kaspi, M. Roberts, and A. K. Harding, in *Compact Stellar X-ray Sources*, edited by W. H. G. Lewin and M. van der Klis (Cambridge University, Cambridge, 2005).

[19] F. Haberl, in *Proceedings of the 2005 EPIC XMM-Newton Consortium Meeting, 2005*, edited by U. G. Briel, S. Sembay, and A. Read, MPE Report 288; e-print astro-ph/0510480.

[20] A. Y. Potekhin, G. Chabrier, and Y. A. Shibanov, *Phys. Rev. E* **60**, 2193 (1999) **63**, 019901(E) (2001).

[21] W. C. G. Ho, D. Lai, A. Y. Potekhin, and G. Chabrier, *Astrophys. J.* **599**, 1293 (2003).

[22] A. Y. Potekhin, D. Lai, G. Chabrier, and W. C. G. Ho, *Astrophys. J.* **612**, 1034 (2004).

[23] D. Lai and E. E. Salpeter, *Astrophys. J.* **491**, 270 (1997).

[24] M. van Adelsberg, D. Lai, A. Y. Potekhin, and P. Arras, *Astrophys. J.* **628**, 902 (2005).

[25] M. D. Jones, G. Ortiz, and D. M. Ceperley, *Phys. Rev. A* **59**, 2875 (1999).

[26] O. A. Al-Hujaj and P. Schmelcher, *Phys. Rev. A* **67**, 023403 (2003).

[27] A. Y. Potekhin, *J. Phys. B* **31**, 49 (1998).

[28] D. Neuhauser, S. E. Koonin, and K. Langanke, *Phys. Rev. A* **36**, 4163 (1987).

[29] K. Mori and C. J. Hailey, *Astrophys. J.* **564**, 914 (2002).

[30] M. V. Ivanov and P. Schmelcher, *Phys. Rev. A* **61**, 022505 (2000).

[31] O. A. Al-Hujaj and P. Schmelcher, *Phys. Rev. A* **70**, 023411 (2004).

[32] O. A. Al-Hujaj and P. Schmelcher, *Phys. Rev. A* **70**, 033411 (2004).

[33] P. Schmelcher, M. V. Ivanov, and W. Becken, *Phys. Rev. A* **59**, 3424 (1999).

[34] I. Fushiki, E. H. Gudmundsson, C. J. Pethick, and J. Yngvason, *Ann. Phys. (N.Y.)* **216**, 29 (1992).

[35] E. H. Lieb, J. P. Solovej, and J. Yngvason, *Commun. Pure Appl. Math.* **47**, 513 (1994).

[36] E. H. Lieb, J. P. Solovej, and J. Yngvason, *Commun. Math. Phys.* **161**, 77 (1994).

[37] P. B. Jones, *Mon. Not. R. Astron. Soc.* **216**, 503 (1985).

[38] P. B. Jones, *Mon. Not. R. Astron. Soc.* **218**, 477 (1986).

[39] D. Kössl, R. G. Wolff, E. Müller, and W. Hillebrandt, *Astron. Astrophys.* **205**, 347 (1988).

[40] B. M. Relovsky and H. Ruder, *Phys. Rev. A* **53**, 4068 (1996).

[41] G. Vignale and M. Rasolt, *Phys. Rev. Lett.* **59**, 2360 (1987).

[42] G. Vignale and M. Rasolt, *Phys. Rev. B* **37**, 10685 (1988).

[43] D. Lai, E. E. Salpeter, and S. L. Shapiro, *Phys. Rev. A* **45**, 4832 (1992).

[44] D. Lai and E. E. Salpeter, *Phys. Rev. A* **53**, 152 (1996).

[45] P. Schmelcher, T. Detmer, and L. S. Cederbaum, *Phys. Rev. A* **64**, 023410 (2001).

[46] G. Ortiz, M. D. Jones, and D. M. Ceperley, *Phys. Rev. A* **52**, R3405 (1995).

[47] M. Demeur, P. H. Heenen, and M. Godefroid, *Phys. Rev. A* **49**, 176 (1994).

[48] Z. Medin and D. Lai, *Phys. Rev. A* **74**, 062508 [the companion paper].

[49] P. Hohenberg and W. Kohn, *Phys. Rev.* **136**, 864 (1964).

[50] W. Kohn and L. J. Sham, *Phys. Rev.* **140**, 1133 (1965).

[51] R. O. Jones and O. Gunnarsson, *Rev. Mod. Phys.* **61**, 689 (1989).

[52] B. B. Kadomtsev and V. S. Kudryavtsev, *Zh. Eksp. Teor. Fiz. Pis'ma Red.* **13**, 61 (1971) [Sov. Phys. JETP **13**, 42 (1971)].

[53] B. B. Kadomtsev, *Zh. Eksp. Teor. Fiz.* **58**, 1765 (1970) [Sov. Phys. JETP **31**, 945 (1970)].

- [54] R. O. Mueller, A. R. P. Rau, and L. Spruch, Phys. Rev. Lett. **26**, 1136 (1971).
- [55] L. D. Landau and E. M. Lifshitz, *Quantum Mechanics* (Pergamon, Oxford, 1977).
- [56] R. W. Danz and M. L. Glasser, Phys. Rev. B **4**, 94 (1971).
- [57] I. Fushiki, E. H. Gudmundsson, and C. J. Pethick, Astrophys. J. **342**, 958 (1989).
- [58] P. Skudlarski and G. Vignale, Phys. Rev. B **48**, 8547 (1993).
- [59] M. Steinberg and J. Ortner, Phys. Rev. B **58**, 15 460 (1998).
- [60] A. M. Abrahams and S. L. Shapiro, Astrophys. J. **382**, 233 (1991).
- [61] W. H. Press, S. A. Teukolsky, W. T. Vetterling, and B. P. Flannery, *Numerical recipes in C. The art of scientific computing* 2nd edition (Cambridge University, Cambridge, 1992).
- [62] J. D. Jackson, *Classical Electrodynamics* 3rd edition (Wiley, New York, 1998).